Hybrid Imaging Using Quantitative $H_2{}^{15}O$ PET and CT-Based Coronary Angiography for the Detection of Coronary Artery Disease

Ibrahim Danad[1], Pieter G. Raijmakers[2], Yolande E. Appelman[1], Hendrik J. Harms[2], Stefan de Haan[1], Mijntje L.P. van den Oever[3], Martijn W. Heymans[4], Igor I. Tulevski[5], Cornelis van Kuijk[3], Otto S. Hoekstra[2], Adriaan A. Lammertsma[2], Mark Lubberink[6], Albert C. van Rossum[1], and Paul Knaapen[1]

[1]Department of Cardiology, VU University Medical Center, Amsterdam, The Netherlands; [2]Department of Nuclear Medicine and PET Research, VU University Medical Center, Amsterdam, The Netherlands; [3]Department of Radiology, VU University Medical Center, Amsterdam, The Netherlands; [4]Department of Epidemiology and Biostatistics, VU University Medical Center, Amsterdam, The Netherlands; [5]Cardiology Centers of The Netherlands, Amsterdam, The Netherlands; and [6]Uppsala University PET Center, Uppsala University Hospital, Uppsala, Sweden

Hybrid imaging using PET in conjunction with CT-based coronary angiography (PET/CTCA) enables near-simultaneous quantification of myocardial blood flow (MBF) and anatomical evaluation of coronary arteries. CTCA is an excellent imaging modality to rule out obstructive coronary artery disease (CAD), but functional assessment is warranted in the presence of a CTCA-observed stenosis because the specificity of CTCA is relatively low. Quantitative $H_2{}^{15}O$ PET/CTCA may yield complementary information and enhance diagnostic accuracy. The purpose of this study was to evaluate the diagnostic accuracy of quantitative $H_2{}^{15}O$ PET/CTCA in a clinical cohort of patients with suspected CAD who underwent both cardiac $H_2{}^{15}O$ PET/CTCA and invasive coronary angiography (ICA). In addition, this study aimed to evaluate and compare the accuracy of hyperemic MBF versus coronary flow reserve (CFR). **Methods:** Patients ($n = 120$; mean age $\pm$ SD, 61 $\pm$ 10 y; 77 men and 43 women) with a predominantly intermediate pretest likelihood for CAD underwent both quantitative $H_2{}^{15}O$ PET/CTCA and ICA. A $\geq$50% stenosis at ICA or a fractional flow reserve $\leq$ 0.80 was considered significant. **Results:** Obstructive CAD was diagnosed in 49 of 120 patients (41%). The diagnostic accuracy of hyperemic MBF was significantly higher than CFR (80% vs. 68%, respectively, $P = 0.02$), with optimal cutoff values of 1.86 mL/min/g and 2.30, respectively. On a per-patient basis, the sensitivity, specificity, negative predictive value, and positive predictive value of CTCA were 100%, 34%, 100%, and 51%, respectively, as compared with 76%, 83%, 83%, and 76%, respectively, for quantitative hyperemic MBF PET. Quantitative $H_2{}^{15}O$ PET/CTCA reduced the number of false-positive CTCA studies from 47 to 6, although 12 of 49 true-positive CTCAs were incorrectly reclassified as false-negative hybrid scans on the basis of (presumably) sufficient hyperemic MBF. Compared with CTCA (61%) or $H_2{}^{15}O$ PET (80%) alone (both $P < 0.05$), the hybrid approach significantly improved diagnostic accuracy (85%). **Conclusion:** The diagnostic accuracy of quantitative $H_2{}^{15}O$ PET/CTCA is superior to either $H_2{}^{15}O$ PET or CTCA alone for the detection of clinically significant CAD. Hyperemic MBF was more accurate than CFR, implying that a single measurement of MBF in diagnostic protocols may suffice.

Key Words: hyperemic MBF; coronary flow reserve; coronary artery disease; diagnostic accuracy; cardiac hybrid $H_2{}^{15}O$ PET/CT

J Nucl Med 2013; 54:55–63
DOI: 10.2967/jnumed.112.104687

Accurate noninvasive assessment of coronary artery disease (CAD) and its functional consequences is a challenging task. There are several cardiac noninvasive imaging techniques, such as SPECT, stress echocardiography, MRI, and PET, for diagnosing and evaluating the extent and severity of myocardial ischemia resulting from CAD. CT coronary angiography (CTCA) has gone through a rapid development during recent years and enables visualization of the coronary artery lumen and wall and provides information about the presence and morphology of coronary artery lesions. Several studies have shown that CTCA accurately rules out obstructive CAD. However, because the positive predictive value (PPV) of CTCA is moderate, functional assessment is also needed in the presence of CTCA-graded obstructive CAD (*1,2*). Approximately half of the lesions deemed obstructive with CTCA are indeed hemodynamically significant as evaluated with fractional flow reserve (FFR) (*3*). Yet the invasive nature of conventional coronary angiography and FFR limits their broad application for initial diagnostic purposes. Therefore, the noninvasive combined assessment of coronary anatomy and perfusion can yield complementary information and may reduce the number of diagnostic invasive coronary angiographies (ICAs) by a more judicious referral of patients to the catheterization lab. The integration of anatomy and function is possible within

Received Feb. 18, 2012; revision accepted Aug. 6, 2012.
For correspondence or reprints contact: Ibrahim Danad, Department of Cardiology, Room 4D36, VU University Medical Center, De Boelelaan 1117, 1081 HV Amsterdam, The Netherlands.
E-mail: i.danad@vumc.nl
Published online Dec. 11, 2012.
COPYRIGHT © 2013 by the Society of Nuclear Medicine and Molecular Imaging, Inc.

a single scan session with the currently available cardiac PET/CT protocols (*4–6*). PET has the unique ability to quantify myocardial blood flow (MBF) in absolute terms, generally with less radiation exposure to the patient, as compared with SPECT (*7*). The quantitative nature of a dynamic PET protocol provides several parameters, such as resting and hyperemic MBF and coronary flow reserve (CFR). In a previous study, Hajjiri et al. demonstrated that hyperemic MBF might be more accurate than CFR or visual defect grading for detecting obstructive CAD (*8*). More recently, in a study by Kajander et al. the combination of quantitative PET (i.e., without visual qualitative grading) and CTCA (PET/CTCA) demonstrated a 95% sensitivity and a 100% specificity and offered a higher diagnostic accuracy than either CTCA or PET alone (*6*). Nonetheless, limited data are available on the accuracy of cardiac quantitative PET/CTCA and the value of hyperemic MBF and CFR for the evaluation of CAD. Therefore, the present study evaluated the accuracy of quantitative $H_2{}^{15}O$ PET/CTCA in a clinical cohort of patients suspected of CAD who underwent both cardiac $H_2{}^{15}O$ PET/CTCA imaging and ICA.

MATERIALS AND METHODS

Patient Population

Data were obtained from a clinical cohort of patients being evaluated for CAD and therefore referred for CTCA, coronary artery calcium (CAC) scoring, and PET MBF measurements on a PET/CT scanner (Gemini TF 64; Philips Healthcare). Patients were referred because of stable (atypical) angina or an elevated risk for CAD (presence of 2 or more risk factors) in the absence of symptoms. Hypertension was defined as a blood pressure of ≥140/90 mm Hg or the use of antihypertensive medication. Hypercholesterolemia was defined as a total cholesterol level of ≥5 mmol/L or treatment with cholesterol-lowering medication. Patients were classified as having diabetes if they were receiving treatment with oral hypoglycemic drugs or insulin. A positive family history of CAD was defined by the presence of CAD in first-degree relatives younger than 55 y in men or 65 y in women. Exclusion criteria were atrial fibrillation, second- or third-degree atrioventricular block, impaired renal function, symptomatic asthma, pregnancy, or a documented history of CAD. A history of CAD was defined as a prior percutaneous coronary intervention, coronary artery bypass graft surgery, or a previous myocardial infarction. Electrocardiography did not show signs of a previous myocardial infarction, and echocardiography showed normal left-ventricular function without wall motion abnormalities in all patients. A total of 120 patients met these criteria and underwent ICA after PET/CTCA (mean interim between studies, 70 d) without a documented cardiac event between PET/CTCA examinations. The indication for ICA was left at the discretion of the referring physician. CAD pretest likelihood was determined according to the criteria of Diamond and Forrester (*9*).

The need for written informed consent was waived by the institutional review board (local ethics committee) because of the nature of the study, which solely had clinical data collection.

PET

The PET/CTCA protocol is shown in Figure 1. The PET sequence has been described in detail previously (*10,11*). Parametric MBF images, showing MBF on the voxel level, were generated, and quantitative analysis was performed using Cardiac VUer software developed in-house (*12*). In short, input functions were obtained using automatic segmentation of dynamic images, after which parametric images were obtained as described previously (*12*). Then, parametric images of perfusable tissue fraction were used for semiautomatic heart segment definition based on the 17-segment model of the American Heart Association (*13*). Obtained volumes of interest were then projected onto dynamic images, and time–activity curves were extracted for each myocardial segment, for each of the 3 vascular territories (right coronary artery [RCA], left anterior descending artery [LAD], and circumflex artery [CX]), and for the entire left ventricle. Finally, segmental and global MBF was calculated using these time–activity curves and nonlinear least squares. MBF was expressed in mL/min/g of perfusable tissue. Two experienced readers masked to the ICA data reviewed all PET scans.

CTCA

Patients with a stable heart rate below 65 bpm (either spontaneous or after the administration of oral or intravenous metoprolol) underwent a CT scan for calcium scoring and CTCA as previously described (*11*). All CT scans were analyzed with a 3-dimensional workstation (Brilliance, Philips) by an experienced radiologist and cardiologist who were masked to the ICA results.

ICA

ICA was performed according to standard clinical protocols. The coronary tree was divided into a 16-segment coronary artery model modified from the American Heart Association (*14*). Significant CAD was defined by a visually graded stenosis ≥ 50%. When FFR measurements were performed, visual grading was overruled by FFR, where a value ≤ 0.80 was considered significant. FFR was measured at the discretion of the interventional cardiolo-

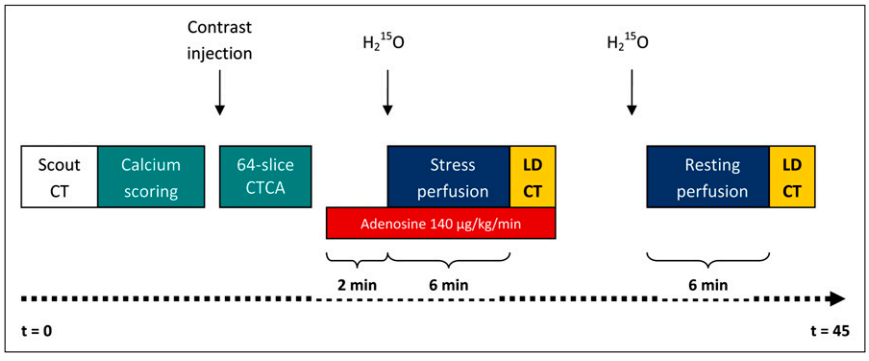

FIGURE 1. Cardiac $H_2{}^{15}O$ PET/CTCA protocol. LD CT = low-dose CT for attenuation correction.

gist performing the ICA procedure. A 0.035-cm (0.014-in) sensor-tipped guide wire (Volcano Corp.) was used, which was introduced through a 6- or 7-French guiding catheter, calibrated, and advanced into the coronary artery. Furthermore, adenosine was infused either intravenously (140 μg/kg/min) or intraarterially (120 μg) in the RCA and left coronary artery, to induce maximal coronary hyperemia. The FFR was calculated as the ratio of the mean distal intracoronary pressure measured by the pressure wire to the mean arterial pressure measured by the coronary catheter (*15*). All images were interpreted by at least 2 experienced interventional cardiologists who were masked to the CTCA and PET data, and subsequently a consensus reading was performed.

Interpretation of Imaging Results

The analysis was performed on both a per-patient and a per-vessel basis. The 4 main vessels—left main artery, LAD, RCA, and left CX—were assessed on CTCA, with stenoses ≥ 50% classified as significant. Comparison of CTCA with ICA or, when available, ICA plus FFR was performed on an intention-to-diagnose basis, and therefore noninterpretable segments on CTCA were considered as significant. In PET, the 3 main vessel regions (LAD, RCA, and left CX) were analyzed. The anatomic information provided by the CTCA scan was used to assess coronary dominance and to allocate a coronary lesion to its subtended vascular territory on the PET perfusion images. In addition, region analysis on a per-segment basis was performed, whereby a perfusion defect of at least 2 adjacent segments was assigned to a vascular territory. Subsequently, this regional perfusion value consisting of at least 2 adjacent segments, instead of the mean MBF of the predefined vascular territory, was used for further analyses. The optimal cutoff values for hyperemic MBF and CFR were calculated using a receiver-operating-characteristic (ROC) curve analysis. A hyperemic MBF ≤ 1.86 mL/min/g and a CFR ≤ 2.30 were considered abnormal (see the "Results" section). The results of PET/CTCA were interpreted as follows. When both CTCA and PET were normal, the vessel was considered normal. A vessel was considered significantly stenosed when a significant stenosis on CTCA was detected in combination with a perfusion abnormality in the region of the corresponding vessel. A vessel was considered nonsignificantly stenosed in the presence of a significant stenosis on CTCA and the absence of a perfusion defect. In the case of a nonsignificant stenosis on CTCA and a perfusion abnormality, the vessel was presumably affected as a result of microvascular dysfunction and was considered nonsignificantly stenosed. Combined anatomic and functional information was gained by mental integration of the information from CTCA and quantitative MBF imaging.

Statistical Analysis

Continuous variables are presented as mean values ± SD, whereas categoric variables are expressed as actual numbers. The performance of PET, CTCA, and PET/CTCA for the diagnosis of CAD, compared with ICA, or when available ICA in combination with FFR measurements, were determined with sensitivity, specificity, negative predictive value (NPV), PPV, and accuracy on a per-patient and per-vessel basis. Furthermore, a head-to-head comparison between hyperemic MBF and CFR was performed to assess the diagnostic accuracy of these PET perfusion parameters.

An ROC curve analysis was used to define optimal cutoff values for hyperemic MBF and CFR in the current study population. A McNemar nonparametric test was used to compare the diagnostic accuracy of CTCA, PET, and PET/CTCA with ICA. A P value ≤ 0.05 was considered statistically significant. All statistical analyses were performed using the SPSS software package (version 16.0; SPSS) and MedCalc (version 11.6.0.0; MedCalc Software).

RESULTS

Patient characteristics (n = 120) are shown in Table 1). In 37 patients, ICA was complemented with a FFR measurement because of the presence of an intermediate coronary lesion. No apparent significant lesion was detected on ICA in 71 patients; 20 of these 71 patients had an ICA in combination with an FFR measurement. Forty-nine patients displayed significant coronary artery stenosis (i.e., ≥50%) at ICA (17 had undergone an FFR measurement). Overall, 92 of the 360 analyzed vessels were graded significant on the basis of visual assessment or FFR measurement. Table 2 summarizes the hemodynamic characteristics. During adenosine-induced hyperemia, only heart rate increased significantly, compared with baseline, whereas no significant changes occurred with respect to blood pressures. Mean heart rate during CTCA was 57 ± 7 beats per minute, which was slightly lower than heart rate during resting perfusion imaging (61 ± 8, $P < 0.01$).

Hyperemic MBF Versus CFR for Detecting Obstructive CAD

The area-under-the-ROC curve (AUC) analysis of hyperemic MBF (AUC, 0.86; 95% confidence interval [CI], 0.81–0.90) was greater than that of CFR (AUC, 0.81; 95% CI, 0.75–0.86) for the detection of obstructive CAD (P = 0.02; Fig. 2). The optimal cutoff values, which were calculated on a per-vessel basis, were ≤1.86 mL/min/g for hyperemic MBF and ≤2.30 for CFR (Fig. 2). The determination

TABLE 1
Patient Characteristics (n = 120)

Characteristic	Value
Sex	
Male	77 (64%)
Female	43 (36%)
Mean age ± SD (y)	61 ± 10
Weight (kg)	83 ± 15
Mean body mass index ± SD (kg/m^2)	28 ± 4
CAD risk factors (*n*)	
Diabetes mellitus	25 (21%)
Hypertension	67 (56%)
Hypercholesterolemia	53 (44%)
Smoking history	55 (46%)
Family history	61 (51%)
Medication (*n*)	
3-hydroxy-3-methyl-glutaryl-CoA reductase inhibitors	94 (78%)
β-blockers	86 (72%)
Aspirin	100 (83%)
Angiotensin-converting enzyme inhibitors	18 (15%)
Angiotensin II receptor blockers	30 (25%)
Calcium channel blockers	45 (38%)
Number of patients with 0/1/2/3 stenotic vessels on ICA	71/22/12/15
Number of FFR measurements	37 (31%)
Pretest likelihood of CAD (%)	55 ± 30
CAC score	442 ± 711

TABLE 2
Hemodynamic Parameters During Scan Procedure

Parameter	Value
Heart rate (bpm)	
Baseline	61 ± 8
Hyperemia	79 ± 13
P, overall difference	<0.001
Systolic blood pressure (mm Hg)	
Baseline	116 ± 19
Hyperemia	116 ± 19
P, overall difference	0.74
Diastolic blood pressure (mm Hg)	
Baseline	61 ± 9
Hyperemia	60 ± 9
P, overall difference	0.32
Mean arterial pressure (mm Hg)	
Baseline	79 ± 11
Hyperemia	78 ± 12
P, overall difference	0.75
Heart rate during CTCA (bpm)	57 ± 7

Data are mean ± SD.

of a cutoff value only in those vessels with obstructive CAD on CTCA revealed that the optimal cutoff value for hyperemic MBF (AUC, 0.83; 95% CI, 0.77–0.89) and CFR (AUC, 0.78; 95% CI, 0.71–0.84) was similar to those obtained in the whole population.

Diagnostic Accuracy of CAC Score, 64-Slice CTCA, and Cardiac PET

The mean CAC score (±SD) in the studied population was 442 ± 711 and was significantly lower in patients without obstructive CAD than in those with obstructive CAD on ICA (359 ± 650 and 564 ± 784, respectively; $P = 0.02$) (Fig. 3). The diagnostic performance of CTCA alone for detecting obstructive CAD on a per-patient and per-vessel basis is displayed in Figures 4 and 5. The sensitivity and NPV of CTCA were excellent (100%), whereas specificity (34%) and PPV (51%) performed poorly in the identification of significant lesions at ICA on a per-patient basis. Similar diagnostic trends were observed on a per-vessel analysis, although specificity increased notably (72%) without an appreciable change in PPV (45%).

Figures 4 and 5 display the diagnostic values for hyperemic MBF and CFR to detect obstructive CAD on a per-patient and per-vessel level. On a per-patient level, sensitivity (76 vs. 76%, $P = 1.00$) was comparable for hyperemic MBF and CFR, whereas specificity (83 vs. 63%, $P < 0.01$) was significantly higher for hyperemic MBF. Hence, total diagnostic accuracy was superior for hyperemic MBF (80 vs. 68%, $P = 0.02$). Comparable results were documented at a per-vessel analysis, as depicted in Figure 5.

Diagnostic Accuracy of Cardiac PET/CTCA

Supplemental Figures 1 and 2 (supplemental materials are available online only at http://jnm.snmjournals.org) show 2 typical examples of cases in which the anatomic lesions on CTCA were as proven functionally significant with PET, which was in concordance with ICA. As depicted in Figure 4A, the combination of CTCA and hyperemic MBF increased specificity (from 34% and 83%, respectively, to 92%; $P < 0.001$ and $P = 0.03$, respectively) and overall diagnostic accuracy (from 61% and 80%, respectively, to 85%; $P < 0.01$ and $P = 0.03$, respectively) in the hybrid protocol on a per-patient basis. However, the high sensitivity of CTCA alone was reduced by adding hyperemic MBF to the hybrid diagnostic evaluation (from 100% and 76%, respectively, to 76%; $P < 0.001$ and $P = 1.00$, respectively); NPV was also reduced (from 100% and 83%, respectively, to 84%; $P < 0.001$ and $P = 1.00$, respectively). Comparable trends were observed when CFR as the perfusion parameter was used

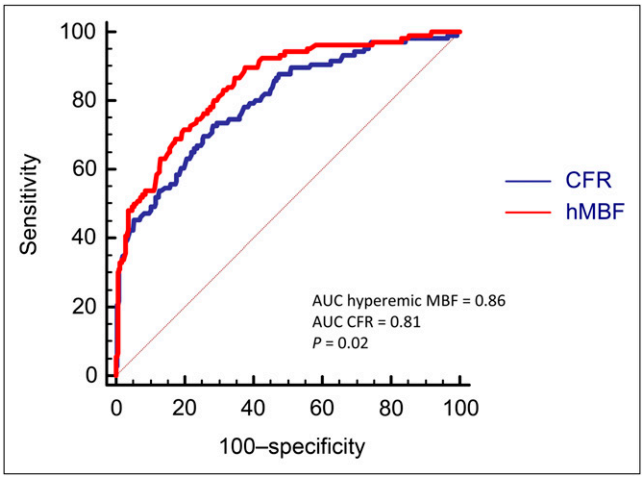

FIGURE 2. Hyperemic MBF vs. CFR for detection of CAD. ROC curves for PET parameters tested for all coronary vessels are shown. CFR = coronary flow reserve; hMBF = hyperemic myocardial blood flow.

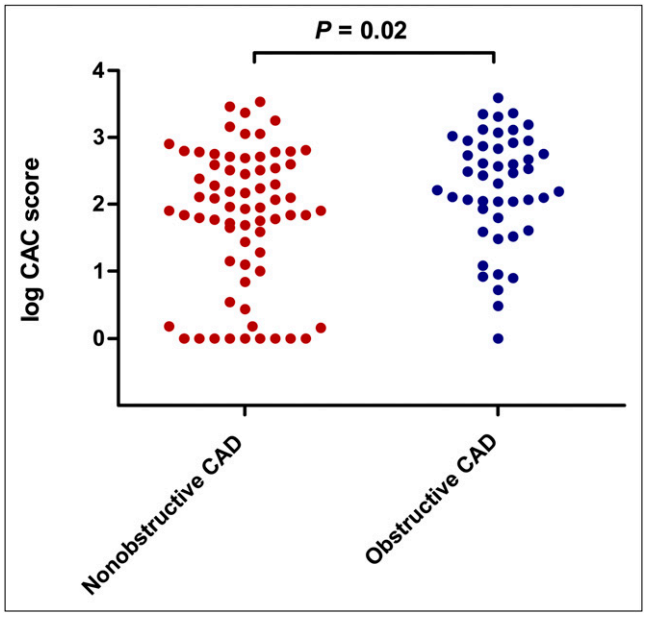

FIGURE 3. Log-transformed CAC score given for patients with and without obstructive CAD on ICA.

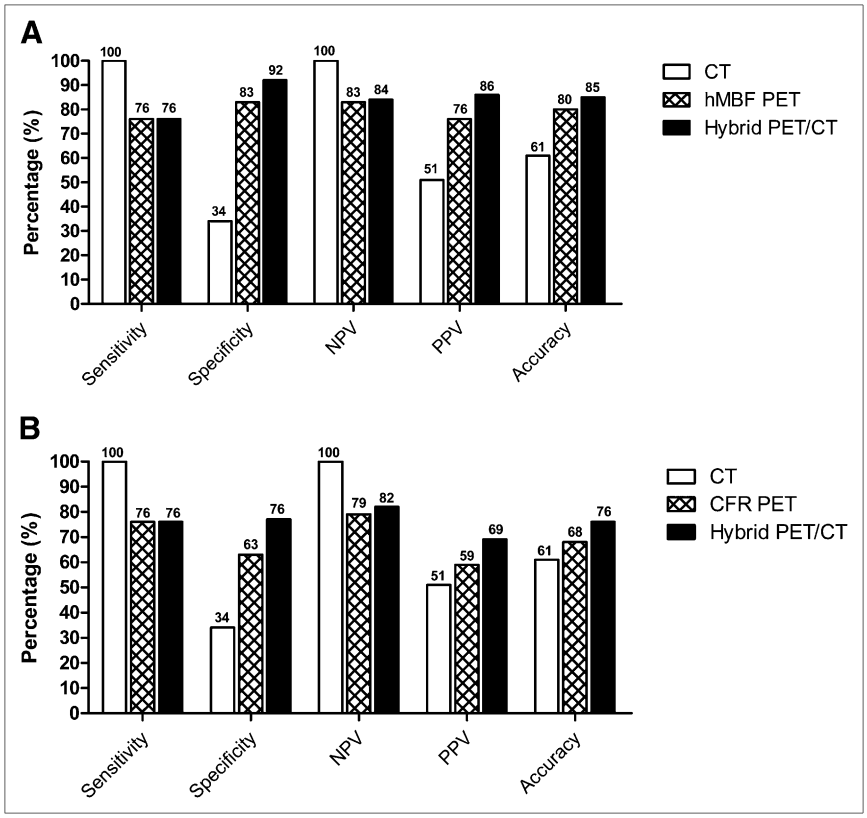

FIGURE 4. Per-patient basis: diagnostic accuracy of noninvasive cardiac imaging. Sensitivity, specificity, NPV, PPV, and accuracy of stand-alone CT, PET, and hybrid imaging. (A) Analysis using hyperemic MBF as perfusion parameter. (B) Analysis using CFR as perfusion parameter. hMBF = hyperemic myocardial blood flow.

in combination with CTCA (Fig. 4B). Overall, hybrid diagnostic accuracy, however, was highest using hyperemic MBF as the perfusion parameter, compared with CFR on a per-patient (85% vs. 76%, $P = 0.04$; Fig. 4) and per-vessel (87 vs. 84%, $P = 0.05$; Fig. 5) analysis. As also listed in Table 3, the hybrid protocol reduced the number of false-positive patients who displayed a stenosis on CTCA in the absence of a significant lesion at ICA (47/71 patients [66%]). Of these 47 patients, 41 were subsequently correctly reclassified as negative on the basis of sufficient hyperemic MBF in all vascular territories. Such a scenario is exemplified in Supplemental Figure 3. For CFR, this correct reclassification number was only 30 (from 47 to 17 patients, Table 4). On the other hand, 12 of 49 CTCA-positive patients (24%) with a least 1 significant lesion at ICA were incorrectly reclassified as negative in the hybrid approach based on (presumably) sufficient hyperemic MBF or CFR in all vascular territories. Supplemental Figure 4 illustrates such a misclassification. Tables 5 and 6 list these results on a per-vessel level, which essentially yielded comparable results.

DISCUSSION

The present study was conducted to evaluate the diagnostic accuracy of quantitative $H_2{}^{15}O$ PET/CTCA for the detection of CAD. The PET perfusion results indicate that hyperemic MBF is superior to CFR and yields a diagnostic accuracy of 80%. Furthermore, combining CTCA with hyperemic MBF in the hybrid protocol enhanced diagnostic accuracy significantly to 85%, mediated through an increase in specificity and PPV as compared with hyperemic MBF alone.

Traditionally, myocardial perfusion imaging for the detection of CAD with PET has been based on qualitative visual grading using $^{13}NH_3$ and ^{82}Rb (static) tracer uptake images. This approach conveys good diagnostic accuracy, and the pooling of data suggests that myocardial perfusion imaging with PET is superior to alternative diagnostic imaging techniques (*16*). Although PET additionally allows for the absolute quantification of MBF, there is a paucity of data on the diagnostic accuracy of hyperemic MBF and CFR. In the present study, hyperemic MBF was superior to CFR in the detection of CAD. Previous studies using quantitative $^{13}NH_3$ PET have shown inconclusive results on this topic. In small-scaled studies, Hajjiri et al. observed a slightly higher accuracy for hyperemic MBF, whereas Muzik et al. concluded that CFR was more accurate, although the differences were small (*8,17*). These observations, in combination with the currently presented data, imply that a single measurement of hyperemic MBF could suffice in diagnostic imaging protocols. The optimal diagnostic cutoff value of 1.86 mL/min/g was in line with the value observed by Hajjiri et al. (1.85 mL/min/g) and somewhat higher than the best discriminatory value documented by Muzik et al. (1.52 mL/min/g), with comparable diagnostic accuracy (AUC ranging from 0.79 to 0.91, compared with 0.86 observed in the present study) (*8,17*). The discriminatory value of

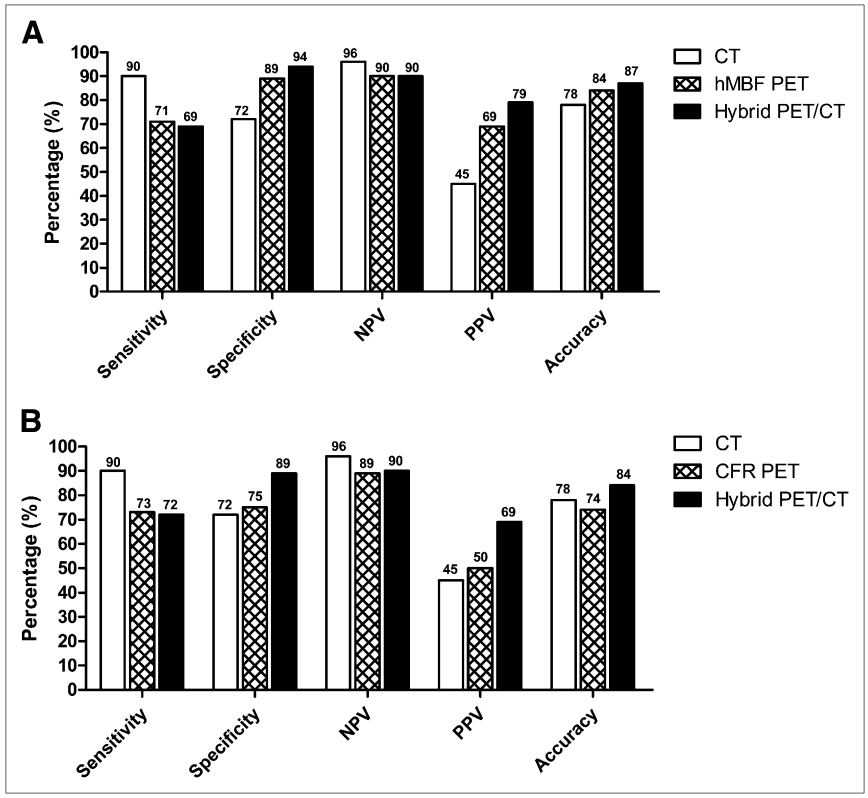

FIGURE 5. Per-vessel basis: diagnostic accuracy of noninvasive cardiac imaging. Sensitivity, specificity, NPV, PPV, and accuracy of stand-alone CT, PET, and hybrid imaging. (A) Analysis using hyperemic MBF as perfusion parameter. (B) Analysis using CFR as perfusion parameter. CFR = coronary flow reserve; hMBF = hyperemic myocardial blood flow.

hyperemic MBF in those patients with obstructive CAD on CTCA was identical to the cutoff value of hyperemic MBF in the entire study population. In contrast, a recent study by Kajander et al., using $H_2{}^{15}O$ PET in 107 patients, displayed an optimal cutoff value of 2.5 mL/min/g with a markedly higher AUC at analysis (0.94) (*6*). Although methodologic considerations between imaging protocols and patient selection may account for some of these discrepancies, the selection of an optimal threshold to reproduce such a high diagnostic yield may prove difficult in clinical practice. Studies in patients without CAD have clearly demonstrated that the reference range of hyperemic MBF is relatively broad because of physiologic variation in minimal coronary microvascular resistance, which is related to patient characteristics such as age, sex, and CAD risk factors (*11,18–20*). Because hyperemic MBF is governed by the (potential) presence of an epicardial coronary lesion and microvascular resistance, a cutoff value to identify an obstructive coronary lesion will vary according to the conductance capacity of the microvascular bed in each individual patient. Indeed, animal experiments using microspheres and several quantitative PET studies using various perfusion tracers in humans have revealed that the relationship between hyperemic MBF and epicardial coronary lesion severity is characterized by considerable scatter (*21–24*). This physiologic variation of hyperemic MBF for a given epicardial coronary lesion hampers the discriminatory power of a single threshold to identify a hemodynamic significant stenosis. The correction of MBF reference values for specific patient subgroups (e.g., age and sex) may improve diagnostic accuracy, although further studies are obviously warranted to test this hypothesis. Although determining an optimal hyperemic MBF cutoff value is rather difficult, the absolute quantification of MBF may provide an added advantage over relative perfusion imaging, particularly in patients with triple-vessel disease or microvascular dysfunction, for whom the relative assessment of coronary perfusion may fail to uncover ischemia due to balanced hypoperfusion.

In line with previous reports, the sensitivity and NPV of CTCA were excellent. Specificity and PPV, however, were

TABLE 3
Results per Patient Using Hyperemic MBF as Perfusion Parameter

Parameter	ICA	
	Positive	Negative
PET/CTCA (n = 120)		
Positive	37	6
Negative	12	65
Hyperemic MBF (n = 120)		
Positive	37	12
Negative	12	59
CTCA (n = 120)		
Positive	49	47
Negative	0	24

In CTCA and PET/CTCA, left main artery, LAD, CX, and RCA were assessed. In PET, LAD, CX, and RCA were analyzed.

TABLE 4
Results per Patient Using CFR as Perfusion Parameter

Parameter	ICA	
	Positive	Negative
PET/CTCA (n = 120)		
Positive	37	17
Negative	12	54
CFR (n = 120)		
Positive	37	26
Negative	12	45
CTCA (n = 120)		
Positive	49	47
Negative	0	24

In CTCA and PET/CTCA, left main artery, LAD, left CX, and RCA were assessed. In PET, LAD, CX, and RCA were analyzed.

moderate and poor, respectively, yielding an overall diagnostic accuracy of 61% on a per-patient basis. Specificity and PPV—even though within the observed range of pooled analysis from multiple studies—appeared to be somewhat lower than generally reported (*25*). That observation was previously documented in a similar clinical cohort of patients (*1,2,26*). Several factors may account for these results, including relatively sensitive grading of coronary plaques at CTCA with a threshold of significance of 50% and an analysis based on an intention to diagnose for which all of the coronary segments were included in the grading, independent of image quality. These results further highlight the general consensus that CTCA is an excellent tool to rule out obstructive CAD, whereas the low PPV warrants further functional testing in the case of a positive CTCA result. In fact, roughly half of lesions deemed positive on CTCA-actually induce myocardial ischemia as documented with SPECT (*27–29*).

The combination of quantitative perfusion assessment with PET and coronary anatomy with CTCA significantly improved the diagnostic accuracy, compared with either imaging technique alone. The hybrid approach was particularly useful to reduce the number of false-positive CTCA findings because the addition of hyperemic MBF could assess the hemodynamic significance of CTCA-observed lesions (Supplemental Fig. 3). On the downside, the excellent sensitivity and NPV of CTCA alone were reduced by the hybrid approach. The latter is the result of an increase in false-negative hybrid scans as illustrated in Supplemental Figure 4.

Overall, these results are in line with previous studies on the diagnostic surplus value of hybrid imaging with PET/CTCA and SPECT/CTCA that consistently display particularly enhanced specificity and PPV with the addition of myocardial perfusion imaging to CTCA (*6,29–32*). Of these studies, only Kajander et al. used quantitative perfusion PET in the hybrid protocol, and thus their study closely resembles the imaging methodology of the current study (*6*). In comparison with Kajander et al., however, the current diagnostic accuracy was lower (85% vs. 98%), with a particular poorer performance regarding sensitivity (76% vs. 95%) and to a lesser extent specificity (92% vs. 100%) on a per-patient basis (*6*). Several methodologic issues may account for this discrepancy. First, and in contrast to Kajander et al., the current study was retrospective, leading to referral bias for which the clinical decision to subject a patient to an invasive coronary angiogram was likely based on an abnormal PET/CTCA finding. Therefore, compared with the study of Kajander et al., the lower diagnostic performance in this study may have been caused by referral bias. Nonetheless, the prevalence of obstructive CAD was similar between studies (both 41%), suggesting that the studied patient populations were comparable. Second, the cutoff values for hyperemic MBF and CFR were not defined a priori but optimized retrospectively using ROC curve analysis in the currently described study population. Prospective trials validating the obtained cutoff values are warranted. Third, FFR measurements were not routinely performed in all patients with an intermediate coronary stenosis. Because agreement between

TABLE 5
Results per Vessel Using Hyperemic MBF as Perfusion Parameter

Parameter	ICA	
	Positive	Negative
PET/CTCA (n = 360)		
Positive	64	17
Negative	29	250
Hyperemic MBF (n = 360)		
Positive	66	29
Negative	27	238
CTCA (n = 480)		
Positive	88	107
Negative	10	275

In CTCA and PET/CTCA, left main artery, LAD, left CX, and RCA were assessed. In PET, LAD, CX, and RCA were analyzed.

TABLE 6
Results per Vessel Using CFR as Perfusion Parameter

Parameter	ICA	
	Positive	Negative
PET/CTCA (n = 360)		
Positive	67	30
Negative	26	237
CFR (n = 360)		
Positive	68	68
Negative	25	199
CTCA (n = 480)		
Positive	88	107
Negative	10	275

In CTCA and PET/CTCA, left main artery, LAD, left CX, and RCA were assessed. In PET, LAD, CX, and RCA were analyzed.

the functional severity of a stenosis as measured with FFR and visual grading may show disparities, the currently used gold standard of invasive angiography is by itself limited (*33*). Fourth, although care was taken to match individual coronary anatomy to perfusion territories in the evaluation of the PET/CTCA scan, software to generate fusion images of CTCA and PET was not commercially available from the manufacturer of our installed system. Some studies have demonstrated that fused hybrid imaging as compared with side-by-side analysis may slightly improve diagnostic accuracy (*34–36*). Finally, parametric perfusion images were generated by different software packages developed in-house in both studies (*12,37*). Although these packages use the same validated single-compartment model to quantify MBF, differences in, for example, arterial input definition and automated myocardial segmentation may cause a systematic bias. This may therefore be related to the observed discrepancy in optimal cutoff value (1.86 vs. 2.5 mL/min/g). Comparative studies between software packages are warranted. Finally, in the current study, $H_2{}^{15}O$, which is not widely available and requires an onsite cyclotron because of its short half-life, was used as a perfusion tracer. In addition, because $H_2{}^{15}O$ water is metabolically inert and freely diffusible, signal-to-noise ratios and contrast between tracer concentration in the blood and in the myocardium is low, compared with other perfusion tracers such as ^{13}N-ammonia and ^{82}Rb. Recently, signal-to-noise ratios of $H_2{}^{15}O$ cardiac PET using blood-pool subtraction techniques have become more sufficient (*37*). Furthermore, generation of high-quality parametric perfusion images is now feasible (*12*). Nonetheless, relative flow imaging with $H_2{}^{15}O$ PET still faces many challenges, and studies investigating the additive value of quantitative MBF imaging, compared with relative flow PET are scarce (*38*). Clearly, more prospective studies are warranted to establish the clinical value of relative perfusion imaging with $H_2{}^{15}O$ as a perfusion tracer.

Irrespective of these methodologic considerations, the results from the current study confirm that quantitative perfusion PET has the ability to diagnose CAD with fairly good accuracy, and PET/CTCA further improves the diagnostic yield. Nonetheless, several important issues remain to be addressed such as whether qualitative or quantitative PET (or their combination) conveys the best results because data on this topic are scarce (*8,38*). The results of prospective studies further exploring the diagnostic accuracy of PET/CTCA are therefore eagerly awaited.

CONCLUSION

Absolute hyperemic MBF measurements with PET are superior to CFR for the diagnosis of obstructive CAD. The addition of CTCA with quantitative PET/CTCA improves diagnostic accuracy significantly.

DISCLOSURE

The costs of publication of this article were defrayed in part by the payment of page charges. Therefore, and solely to indicate this fact, this article is hereby marked "advertisement" in accordance with 18 USC section 1734. No other potential conflict of interest relevant to this article was reported.

ACKNOWLEDGMENTS

We thank Suzette van Balen, Amina Elouahmani, Judith van Es, Robin Hemminga, Femke Jongsma, Nghi Pham, and Nasserah Sais for performing the scans and Henri Greuter, Marissa Rongen, Robert Schuit, and Kevin Takkenkamp for producing ^{15}O-water.

REFERENCES

1. Meijboom WB, Meijs MF, Schuijf JD, et al. Diagnostic accuracy of 64-slice computed tomography coronary angiography: a prospective, multicenter, multivendor study. *J Am Coll Cardiol.* 2008;52:2135–2144.
2. Budoff MJ, Dowe D, Jollis JG, et al. Diagnostic performance of 64-multidetector row coronary computed tomographic angiography for evaluation of coronary artery stenosis in individuals without known coronary artery disease: results from the prospective multicenter ACCURACY (Assessment by Coronary Computed Tomographic Angiography of Individuals Undergoing Invasive Coronary Angiography) trial. *J Am Coll Cardiol.* 2008;52:1724–1732.
3. Meijboom WB, Van Mieghem CA, van Pelt N, et al. Comprehensive assessment of coronary artery stenoses: computed tomography coronary angiography versus conventional coronary angiography and correlation with fractional flow reserve in patients with stable angina. *J Am Coll Cardiol.* 2008;52:636–643.
4. Knaapen P, de Haan S, Hoekstra OS, et al. Cardiac PET-CT: advanced hybrid imaging for the detection of coronary artery disease. *Neth Heart J.* 2010;18:90–98.
5. Di Carli MF, Hachamovitch R. New technology for noninvasive evaluation of coronary artery disease. *Circulation.* 2007;115:1464–1480.
6. Kajander S, Joutsiniemi E, Saraste M, et al. Cardiac positron emission tomography/computed tomography imaging accurately detects anatomically and functionally significant coronary artery disease. *Circulation.* 2010;122:603–613.
7. Radiation dose to patients from radiopharmaceuticals (addendum 2 to ICRP publication 53). *Ann ICRP.* 1998;28:1–126.
8. Hajjiri MM, Leavitt MB, Zheng H, Spooner AE, Fischman AJ, Gewirtz H. Comparison of positron emission tomography measurement of adenosine-stimulated absolute myocardial blood flow versus relative myocardial tracer content for physiological assessment of coronary artery stenosis severity and location. *JACC Cardiovasc Imaging.* 2009;2:751–758.
9. Diamond GA, Forrester JS. Analysis of probability as an aid in the clinical diagnosis of coronary-artery disease. *N Engl J Med.* 1979;300:1350–1358.
10. Lubberink M, Harms HJ, Halbmeijer R, de Haan S, Knaapen P, Lammertsma AA. Low-dose quantitative myocardial blood flow imaging using ^{15}O-water and PET without attenuation correction. *J Nucl Med.* 2010;51:575–580.
11. Danad I, Raijmakers PG, Appelman YE, et al. Coronary risk factors and myocardial blood flow in patients evaluated for coronary artery disease: a quantitative [(15)O]H (2)O PET/CT study. *Eur J Nucl Med Mol Imaging.* 2012;39:102–112.
12. Harms HJ, Knaapen P, de Haan S, Halbmeijer R, Lammertsma AA, Lubberink M. Automatic generation of absolute myocardial blood flow images using [^{15}O]H2O and a clinical PET/CT scanner. *Eur J Nucl Med Mol Imaging.* 2011;38:930–939.
13. Cerqueira MD, Weissman NJ, Dilsizian V, et al. Standardized myocardial segmentation and nomenclature for tomographic imaging of the heart: a statement for healthcare professionals from the Cardiac Imaging Committee of the Council on Clinical Cardiology of the American Heart Association. *Circulation.* 2002;105:539–542.
14. Austen WG, Edwards JE, Frye RL, et al. A reporting system on patients evaluated for coronary artery disease: report of the Ad Hoc Committee for Grading of Coronary Artery Disease, Council on Cardiovascular Surgery, American Heart Association. *Circulation.* 1975;51:5–40.
15. Pijls NH, De Bruyne B, Peels K, et al. Measurement of fractional flow reserve to assess the functional severity of coronary-artery stenoses. *N Engl J Med.* 1996;334:1703–1708.
16. Nandalur KR, Dwamena BA, Choudhri AF, Nandalur SR, Reddy P, Carlos RC. Diagnostic performance of positron emission tomography in the detection of coronary artery disease: a meta-analysis. *Acad Radiol.* 2008;15:444–451.
17. Muzik O, Duvernoy C, Beanlands RS, et al. Assessment of diagnostic performance of quantitative flow measurements in normal subjects and patients with angiographically

documented coronary artery disease by means of nitrogen-13 ammonia and positron emission tomography. *J Am Coll Cardiol.* 1998;31:534–540.
18. Chareonthaitawee P, Kaufmann PA, Rimoldi O, Camici PG. Heterogeneity of resting and hyperemic myocardial blood flow in healthy humans. *Cardiovasc Res.* 2001;50:151–161.
19. Duvernoy CS, Meyer C, Seifert-Klauss V, et al. Gender differences in myocardial blood flow dynamics: lipid profile and hemodynamic effects. *J Am Coll Cardiol.* 1999;33:463–470.
20. Wang L, Jerosch-Herold M, Jacobs DR Jr, Shahar E, Folsom AR. Coronary risk factors and myocardial perfusion in asymptomatic adults: the Multi-Ethnic Study of Atherosclerosis (MESA). *J Am Coll Cardiol.* 2006;47:565–572.
21. Anagnostopoulos C, Almonacid A, El Fakhri G, et al. Quantitative relationship between coronary vasodilator reserve assessed by ^{82}Rb PET imaging and coronary artery stenosis severity. *Eur J Nucl Med Mol Imaging.* 2008;35: 1593–1601.
22. Gould KL, Lipscomb K. Effects of coronary stenoses on coronary flow reserve and resistance. *Am J Cardiol.* 1974;34:48–55.
23. Uren NG, Melin JA, de Bruyne B, Wijns W, Baudhuin T, Camici PG. Relation between myocardial blood flow and the severity of coronary-artery stenosis. *N Engl J Med.* 1994;330:1782–1788.
24. Di Carli M, Czernin J, Hoh CK, et al. Relation among stenosis severity, myocardial blood flow, and flow reserve in patients with coronary artery disease. *Circulation.* 1995;91:1944–1951.
25. Paech DC, Weston AR. A systematic review of the clinical effectiveness of 64-slice or higher computed tomography angiography as an alternative to invasive coronary angiography in the investigation of suspected coronary artery disease. *BMC Cardiovasc Disord.* 2011;11:32.
26. Groothuis JG, Beek AM, Meijerink MR, et al. Positive predictive value of computed tomography coronary angiography in clinical practice. *Int J Cardiol.* 2012;156:315–319.
27. Gaemperli O, Schepis T, Valenta I, et al. Functionally relevant coronary artery disease: comparison of 64-section CT angiography with myocardial perfusion SPECT. *Radiology.* 2008;248:414–423.
28. Schuijf JD, Wijns W, Jukema JW, et al. Relationship between noninvasive coronary angiography with multi-slice computed tomography and myocardial perfusion imaging. *J Am Coll Cardiol.* 2006;48:2508–2514.
29. Rispler S, Keidar Z, Ghersin E, et al. Integrated single-photon emission computed tomography and computed tomography coronary angiography for the assessment of hemodynamically significant coronary artery lesions. *J Am Coll Cardiol.* 2007;49:1059–1067.
30. Namdar M, Hany TF, Koepfli P, et al. Integrated PET/CT for the assessment of coronary artery disease: a feasibility study. *J Nucl Med.* 2005;46:930–935.
31. Groves AM, Speechly-Dick ME, Kayani I, et al. First experience of combined cardiac PET/64-detector CT angiography with invasive angiographic validation. *Eur J Nucl Med Mol Imaging.* 2009;36:2027–2033.
32. Sato A, Nozato T, Hikita H, et al. Incremental value of combining 64-slice computed tomography angiography with stress nuclear myocardial perfusion imaging to improve noninvasive detection of coronary artery disease. *J Nucl Cardiol.* 2010;17:19–26.
33. Tonino PA, Fearon WF, de Bruyne B, et al. Angiographic versus functional severity of coronary artery stenoses in the FAME study fractional flow reserve versus angiography in multivessel evaluation. *J Am Coll Cardiol.* 2010;55:2816–2821.
34. Gaemperli O, Schepis T, Valenta I, et al. Cardiac image fusion from stand-alone SPECT and CT: clinical experience. *J Nucl Med.* 2007;48:696–703.
35. Santana CA, Garcia EV, Faber TL, et al. Diagnostic performance of fusion of myocardial perfusion imaging (MPI) and computed tomography coronary angiography. *J Nucl Cardiol.* 2009;16:201–211.
36. Slomka PJ, Cheng VY, Dey D, et al. Quantitative analysis of myocardial perfusion SPECT anatomically guided by coregistered 64-slice coronary CT angiography. *J Nucl Med.* 2009;50:1621–1630.
37. Nesterov SV, Han C, Maki M, et al. Myocardial perfusion quantitation with ^{15}O-labelled water PET: high reproducibility of the new cardiac analysis software (Carimas). *Eur J Nucl Med Mol Imaging.* 2009;36:1594–1602.
38. Kajander SA, Joutsiniemi E, Saraste M, et al. Clinical value of absolute quantification of myocardial perfusion with ^{15}O-water in coronary artery disease. *Circ Cardiovasc Imaging.* 2011;4:678–684.